Available online at www.sciencedirect.com
ScienceDirect
Ocean Engineering 35 (2008) 47–52
OCEAN ENGINEERING
www.elsevier.com/locate/oceaneng

Steepness and spectrum of nonlinear deformed shallow water wave

Narcisse Zahibo[a], Irina Didenkulova[b,c], Andrey Kurkin[b], Efim Pelinovsky[b,c,*]

[a] *Physics Department, University of Antilles Guyane, Pointe-a-Pitre, Guadeloupe, France*
[b] *Applied Mathematics Department, State Technical University, Nizhny Novgorod, Russia*
[c] *Department of Nonlinear Geophysical Processes, Institute of Applied Physics, Nizhny Novgorod, Russia*

Received 28 June 2007; accepted 1 July 2007
Available online 10 July 2007

Abstract

The process of the nonlinear deformation of a shallow water wave in a basin of a constant depth is studied. Characteristics of the first breaking of the wave are analyzed in detail. The Fourier spectrum and steepness of the nonlinear wave are calculated. It is shown that the spectral amplitudes can be expressed using the wave front steepness, which allows the practical estimations.

Keywords: Nonlinear deformation; Wave breaking; Fourier spectrum; Steepness; Shallow water theory

1. Introduction

The process of the nonlinear wave evolution in the shallow water resulting in wave breaking is well known, and it can be described analytically in the framework of the nonlinear shallow-water theory (see, for instance, books: Stoker, 1957; Whitham, 1974; Engelbrecht et al., 1988; Voltsinger et al., 1989; Arseniev and Shelkovnikov, 1991; Tan, 1992). Mathematically, wave breaking can be considered as the crossing of the characteristics of the hyperbolic system for the shallow water (gradient catastrophe). Many observations of wave breaking and its transformation into an undular bore were made during the huge tsunami in the Indian Ocean which occurred on 26 December 2004 after the earthquake with magnitude of 9.3. Fig. 1 shows a set of photos taken by a Canadian couple of the tsunami approaching the coast (these photos have subsequently been shown on TV very often). The increase in the steepness of the tsunami wave front can also be obtained by numerical simulation of the tsunami wave propagation on long distances (Zahibo et al., 2006) and predicted theoretically (Hammack, 1973; Ostrovsky and Pelinovsky, 1976; Murty, 1977; Pelinovsky, 1982). This phenomenon of steepness increase is also observed when sea waves enter the river mouths (Pelinovsky, 1982; Tsuji et al., 1991), straits, or channels (Pelinovsky and Troshina, 1994; Wu and Tian, 2000; Caputo and Stepanyants, 2003). Meanwhile, we do not know of any publications, where the characteristics of the nonlinear deformed wave such as steepness, spectrum and location of the breaking point have been analyzed in detail. In this paper, we shall analyze the nonlinear deformation of the shallow water wave in a basin of a constant depth without wave amplitude limitation. This article is organized as follows. In Section 2, the spatial evolution of the nonlinear deformed wave and the characteristics of the first breaking are analyzed. In Section 3, the wave steepness and the Fourier spectrum of the nonlinear deformed periodic wave are studied. In Section 4 we present the conclusions.

2. Spatial evolution of the shallow water wave

The basic equations of the nonlinear shallow water theory can be written in the following form (Stoker, 1955):

$$\frac{\partial u}{\partial t} + u\frac{\partial u}{\partial x} + g\frac{\partial \eta}{\partial x} = 0, \qquad (1)$$

$$\frac{\partial \eta}{\partial t} + \frac{\partial}{\partial x}[(h+\eta)u] = 0,$$

*Corresponding author. Department of Nonlinear Geophysical Processes, Institute of Applied Physics, Russian Academy of Sciences, 46 Uljanov Street, Nizhny Novgorod, Russia. Tel.: +7 8314 164839; fax: +7 8314 365976.
E-mail address: pelinovsky@hydro.appl.sci-nnov.ru (E. Pelinovsky).

0029-8018/$ - see front matter © 2007 Elsevier Ltd. All rights reserved.
doi:10.1016/j.oceaneng.2007.07.001

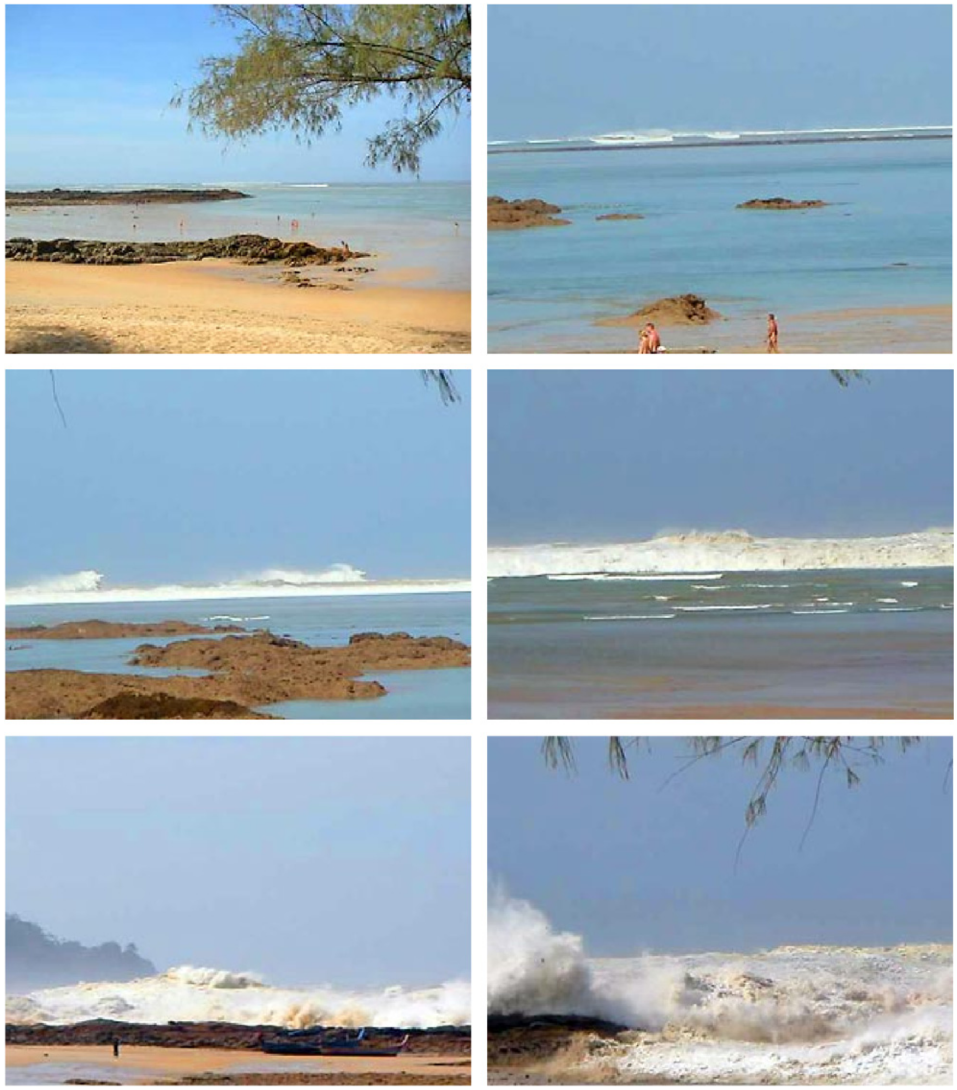

Fig. 1. Snapshot of tsunami approaching the coast (Indian Ocean, December 26, 2004).

where η is the water level displacement, u is the horizontal velocity of water flow, g is the gravitational acceleration and h is the unperturbed water depth assumed to be constant.

In the unidirectional wave, the flow velocity depends on the water displacement only, and after substitution $u = u(\eta)$ in (1), the relation between u and η can be found explicitly by

$$u = 2\left(\sqrt{g(h+\eta)} - \sqrt{gh}\right) \tag{2}$$

(for definiteness, we consider waves propagating in the positive direction, $x>0$). Using this assumption, (1) can be reduced to the first-order quasi-linear partial differential equation (Whitham, 1974; Voltsinger et al., 1989)

$$\frac{\partial \eta}{\partial t} + V(\eta)\frac{\partial \eta}{\partial x} = 0, \tag{3}$$

where the wave speed (or characteristic speed) V is

$$V(\eta) = 3\sqrt{g(h+\eta)} - 2\sqrt{gh}. \tag{4}$$

It is important to mention that Eq. (3) is an exact equation and it is valid formally for the waves of an arbitrary amplitude if dispersion and dissipation are neglected.

We will solve Eq. (3) with boundary condition $\eta(t, x=0) = \eta_0(t)$, which is typical for the cases when the wave is generated in the laboratory tank by the wavemaker. Thus, the solution of Eq. (3) is

$$\eta(x,t) = \eta_0\left(t - \frac{x}{V(\eta)}\right), \quad \text{or} \quad t - \frac{x}{V(\eta)} = \tau(\eta), \tag{5}$$

where $\tau(\eta)$ is an inverse function to $\eta_0(t)$ which is determined by the wavemaker. First of all, it is important to mention that the wave may propagate from the wavemaker in the positive direction $x>0$ only if

$$\eta > -\frac{5}{9}h, \tag{6}$$

and, therefore, the wave trough should not be deep.

The implicit formula (5) describes a simple or Riemann wave, which is well known in nonlinear acoustics (Rudenko and Soluyan, 1977; Engelbrecht et al., 1988; Gurbatov et al., 1991). This solution describes the nonlinear deformation of the wave with distance; the steepness of its face slope increases with distance. The time derivative of the wave profile can be calculated in the explicit form

$$\frac{\partial \eta}{\partial t} = \frac{d\eta_0/d\tau}{1 + x\, dV^{-1}(\eta_0)/d\tau}. \tag{7}$$

On the face slope ($\partial\eta/\partial t > 0$) the time derivative dV^{-1}/dt is negative, and the denominator in (6) decreases with distance; the time derivative of the wave profile increases and tends to infinity at distance $x = X$. The breaking length (nonlinearity length) which characterizes the first breaking equals to

$$X = \frac{1}{\max(-dV^{-1}/dt)}. \tag{8}$$

Therefore, the wave begins to break at the point on the wave profile where the inverse speed derivative reaches its maximum, and this point in general does not coincide with the point of the wave profile with the maximum steepness. As a detailed example, the initial sinusoidal shape of the generated wave will be analyzed. Such a wave, $\eta_0(t) = a\sin(\omega t)$, has the maximum derivative equal to $a\omega$ in the wave point with the zero displacement of the water level. The breaking begins in the trough, and the phase ($\theta = \omega t_*$) and displacement ($\zeta = \eta_*/h$, $\eta_* = a\sin\theta$) of the breaking point (see Fig. 2 for definitions) depend on the wave amplitude ($A = a/h$) through the algebraic dimensionless expressions

$$A = \sqrt{\frac{\zeta^2(3\sqrt{1+\zeta}+2) - 2\zeta(3\sqrt{1+\zeta}-2)}{9\sqrt{1+\zeta}-2}},$$
$$\theta = \arcsin\left(\frac{\zeta}{A}\right). \tag{9}$$

These characteristics are shown in Figs. 3 and 4. At small wave amplitudes the first breaking appears in the wave on the zero level (unperturbed fluid surface), and in this case the following asymptotic formulas can be used to estimate displacement and phase of the breaking point:

$$\zeta \approx -\frac{7}{2}A^2, \quad \theta \approx -\frac{7}{2}A. \tag{10}$$

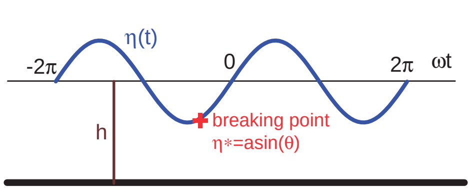

Fig. 2. Location of the breaking point in trough on the shallow-water wave.

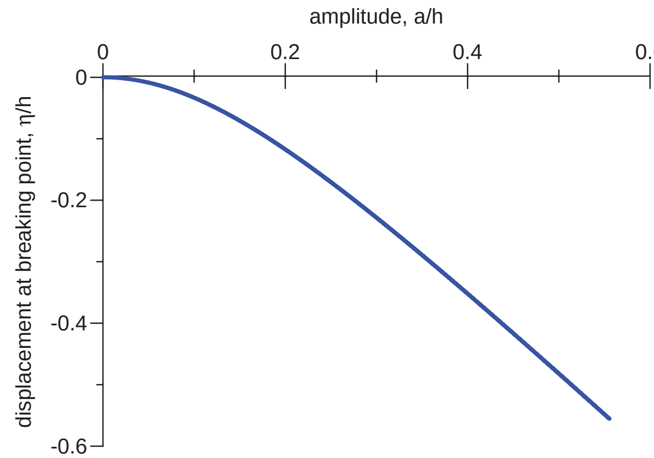

Fig. 3. Displacement at the breaking point versus the wave amplitude.

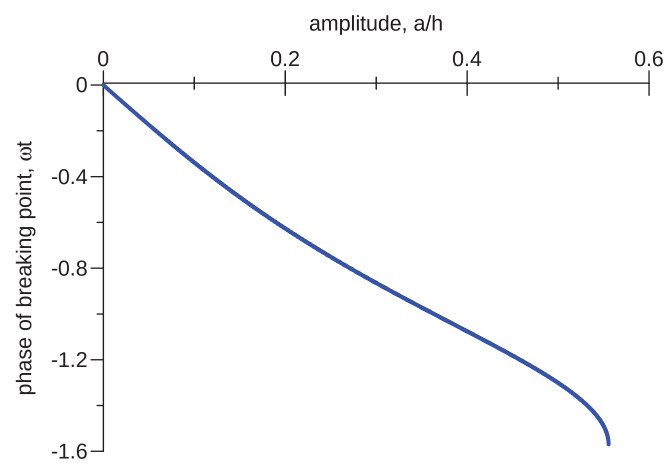

Fig. 4. Phase of the breaking point versus the wave amplitude.

When the wave amplitude approaches the critical value (6), the breaking point shifts to the end of the wave trough

$$\zeta \approx -A = \frac{5}{9}, \quad \theta \approx -\frac{\pi}{2}. \tag{11}$$

The distance the wave travels from the wavemaker to the breaking point (breaking length) can be found from (8)

$$\omega T = \frac{2\sqrt{1+\zeta}(3\sqrt{1+\zeta}-2)^2}{3A\ \cos\ \theta}, \tag{12}$$

where expressions (9) should be used. In fact, we introduce the breaking time, $T = X/(gh)^{1/2}$ reducing the number of the dimensional quantities. The breaking time decreases when the wave amplitude increases (Fig. 5) and tends to zero as the wave amplitude tends to its critical value 5/9. Thus, the wave of large amplitude breaks near the wavemaker and in fact does not propagate. For weak amplitude waves the breaking time is big, and it can be described by the asymptotic formula

$$\omega T \approx \frac{2}{3A}. \tag{13}$$

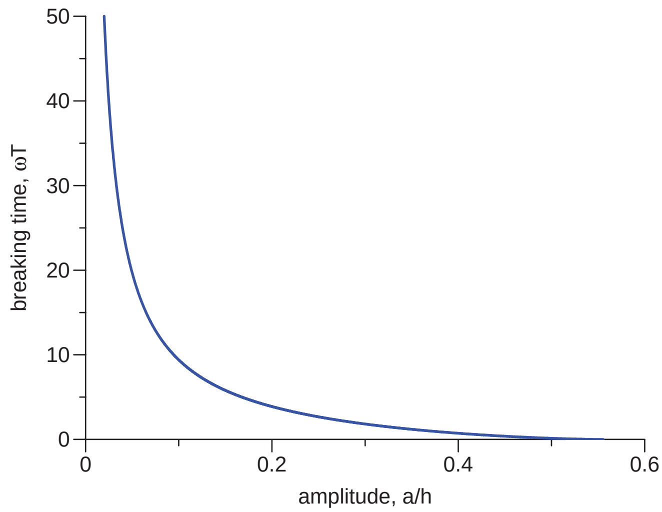

Fig. 5. Breaking time versus the wave amplitude.

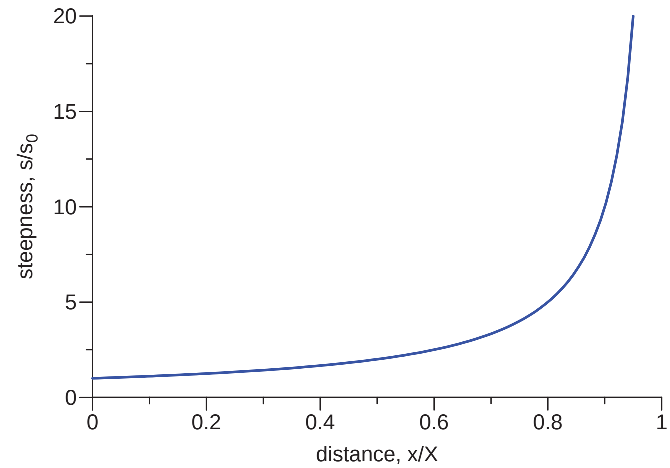

Fig. 6. The wave steepness versus the distance from the wavemaker.

Taking into the account the importance of this formula for practice let us give it in a dimensional form

$$X = \frac{2\sqrt{gh}h}{3\omega a} = \frac{\lambda h}{3\pi a}, \tag{14}$$

where the wavelength λ is determined by the linear dispersion relation of long waves,

$$\lambda = \frac{2\pi\sqrt{gh}}{\omega}. \tag{15}$$

The weak amplitude wave has to propagate a long distance of many wavelengths before the nonlinear effects become significant and the wave breaks.

3. The wave steepness and Fourier spectrum

The wave steepness is the measured characteristics of the wave field important for applications, and it can be calculated exactly from (5)

$$\frac{\partial\eta}{\partial x} = -\frac{1}{V}\frac{\partial\eta}{\partial t} = -\frac{V^{-1}(\eta_0)\mathrm{d}\eta_0/\mathrm{d}\tau}{1 + x\mathrm{d}V^{-1}(\eta_0)/\mathrm{d}\tau}. \tag{16}$$

The maximum steepness is achieved at the point of wave profile where V^{-1} has the maximum time derivative; the first breaking occurs at this point. Taking into the account the definition of the breaking length (8) from (16) follows the expression for maximum steepness

$$s = \max(\partial\eta/\partial x) = \frac{s_0}{1 - x/X}, \tag{17}$$

where $s_0 = \partial\eta_0/\partial x = V^{-1}\partial\eta_0/\partial t$ is the initial steepness of the wave in the point η_*. The maximum steepness increases very rapidly in the vicinity of the breaking point, see Fig. 6. The minimum steepness is achieved on the back face of the wave, and it is varied with distance as

$$s_{\min} = \min(\partial\eta/\partial x) = \frac{s_0}{1 + x/X}. \tag{18}$$

The minimum steepness reduces with distance and it is half of the initial steepness at the breaking point. The steepness of the nonlinear deformed wave can be calculated similarly for other points on the wave profile.

For practice it is important to know the frequency spectrum of the wave field. In general form the Fourier integral can be written in the explicit form (Pelinovsky, 1976)

$$S(\omega) = \int \eta(x,t)\exp(-\mathrm{i}\omega t)\,\mathrm{d}t = \frac{1}{i\omega}\int \frac{\mathrm{d}\eta_0}{\mathrm{d}\tau}\exp(-\mathrm{i}\omega[\tau + x/V(\eta_0)])\,\mathrm{d}\tau \tag{19}$$

It is impossible to calculate this integral analytically even for monochromatic initial disturbances. Let us consider here, the case of weak, but finite amplitudes when the wave propagates on long distances without breaking. Using the Taylor's series for inverse velocity $V^{-1}(\eta) = (gh)^{-1/2}(1–3\eta/2h)$, integral (19) can be calculated exactly and the wave field at any distance from the wavemaker is

$$\eta(t,x) = \sum_{n=1}^{\infty} A_n(x)\sin\left(n\omega[t - x/\sqrt{gh}]\right) = \frac{4h\sqrt{gh}}{3\omega x}\sum_{n=1}^{\infty}\frac{1}{n}J_n\left(\frac{3n\omega x a}{2h\sqrt{gh}}\right) \times \sin\left(n\omega[t - x/\sqrt{gh}]\right), \tag{20}$$

where J_n is the Bessel function of nth order. Spectral amplitudes can be re-written in the following form using the same accuracy for the breaking length (14):

$$A_n(x) = 2a\frac{X}{nx}J_n\left(\frac{nx}{X}\right). \tag{21}$$

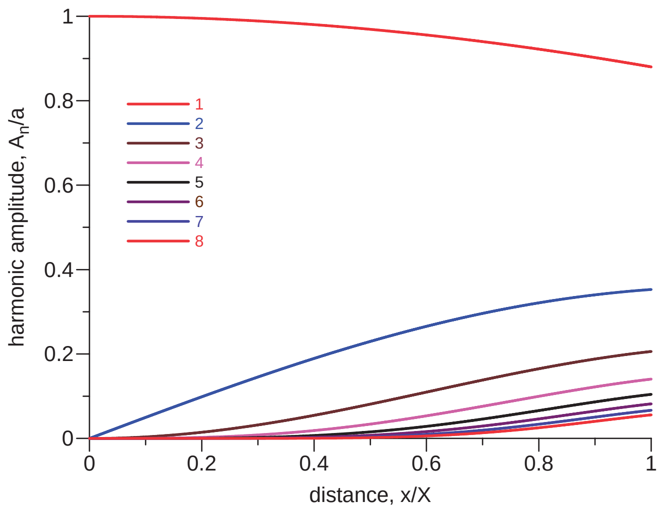

Fig. 7. Harmonic amplitudes versus the distance from the wavemaker (first to eighth harmonics are displayed from the top).

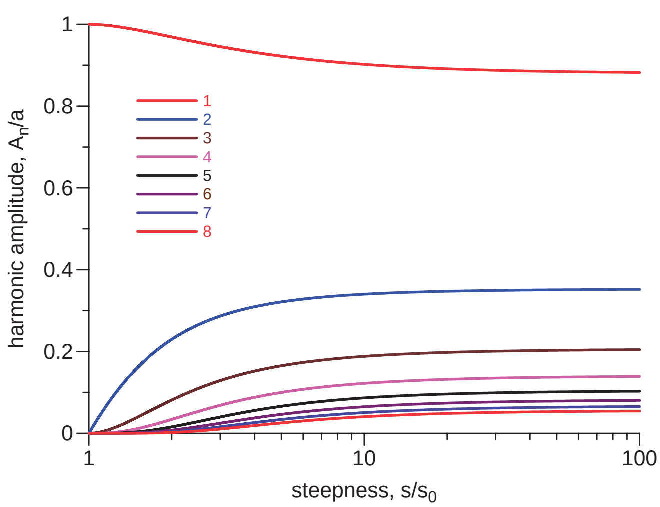

Fig. 8. Harmonic amplitudes versus maximum wave steepness from the top.

The amplitudes of high harmonics grow with distance from the wavemaker, and the amplitude of basic harmonics decreases with distance from the wavemaker because the energy transfers to the high harmonics (Fig. 7). It is important to mention that harmonic amplitudes are relatively weak even at the breaking point and decrease with the increase in harmonic number.

In oceanic conditions the distance from the wave source is unknown. It is more useful to have the relationship between the harmonic amplitudes and the wave steepness. Using (17) for maximum steepness, formula (21) can be written as

$$A_n(s) = \frac{2a}{n(1 - s_0/s)} J_n\left(n\left[1 - \frac{s_0}{s}\right]\right). \tag{22}$$

The relationship between the harmonic amplitudes and wave steepness is displayed in Fig. 8.

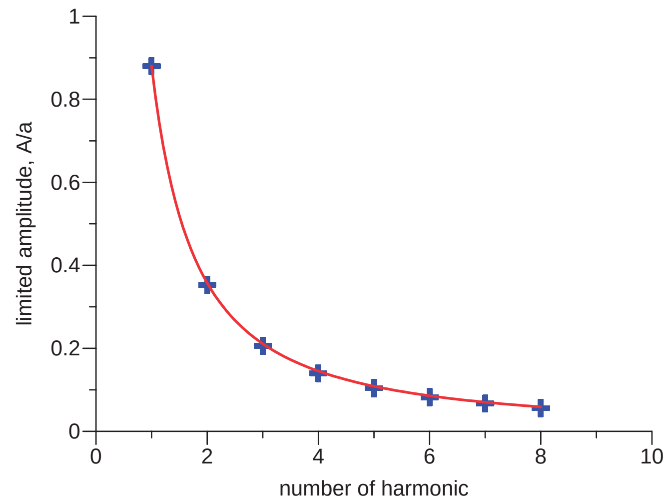

Fig. 9. Limited spectrum of the shallow-water wave in the vicinity of the breaking point (solid line—asymptotic $n^{-1.3}$).

It can be observed that for large values of the wave steepness the harmonic amplitudes tend to constant values. This limited spectrum of the shallow water wave (see Fig. 9) does not depend on the initial wave steepness

$$\bar{A}_n = \frac{2a}{n} J_n(n). \tag{23}$$

This function is very well approximated by the power asymptotic, $n^{-1.3}$, presented in Fig. 9 by a solid line. The spectrum of the nonlinear nondispersive wave field has been theoretically studied in Gurbatov et al., (1991) in detail. According to the theory, the asymptotic $\omega^{-3/2}$ appears in the vicinity of the breaking point and this is close to the approximated curve (23) calculated for the periodic waves. After the wave breaking, the asymptotic ω^{-1} in high-frequency range forms; this corresponds to the "jump" functions.

4. Conclusion

The behavior of the nonlinear shallow-water wave generated by the wavemaker is discussed within the framework of the exact solution in the form of the Riemann (simple) wave. It is shown that the initial sinusoidal wave can propagate as the smooth wave only if its amplitude is consistent with condition $a < 5h/9$, where h is water depth. The wave begins to break at the point on the wave profile where the local value of the inverse velocity of propagation is maximal. The breaking length is calculated; it decreases when the wave amplitude increases. The steepness and the spectrum of the nonlinear deformed wave are calculated in the explicit form. The spectral amplitudes of the wave harmonics can be expressed in terms of the local value of the maximum steepness of the wave front. The Fourier spectrum has the universal shape for very steep waves. These estimates of the wave spectrum can be used in the engineering practice.

Acknowledgments

This study was supported in particular by Grants from INTAS (03-51-4286 and, 06-1000013-9236 and 06-1000014-6046) and RFBR (05-05-64265 and 06-05-91553).

References

Arseniev, A.C., Shelkovnikov, N.K., 1991. Dynamics of Sea Long Waves. Moscow State University Press, Moscow (in Russian).

Caputo, J.-G., Stepanyants, Y.A., 2003. Bore formation, evolution and disintegration into solitons in shallow inhomogeneous channels. Nonlinear Processes in Geophysics 10, 407–424.

Engelbrecht, J.K., Fridman, V.E., Pelinovski, E.N., 1988. Nonlinear Evolution Equations, (Pitman Research Notes in Mathematics Series, No. 180). Longman, London.

Gurbatov, S., Malakhov, A., Saichev, A., 1991. Nonlinear Random Waves and Turbulence in Nondispersive Media: Waves, Rays and Particles. Manchester University Press, Manchester.

Hammack, J.L., 1973. A note on tsunamis: their generation and propagation in an ocean of uniform depth. Journal of Fluid Mechanics 60, 769–799.

Murty, T., 1977. Seismic sea waves—Tsunamis. Canada.

Ostrovsky, L., Pelinovsky, E., 1976. Nonlinear evolution of tsunami waves. Bulletin of the Royal Society of New Zealand 15, 203–211.

Pelinovsky, E.N., 1976. Spectral analysis of simple waves. Radiophysics and Quantum Electronics 19 (3), 262–270.

Pelinovsky, E.N., 1982. Nonlinear Dynamics of Tsunami Waves. Applied Physical Institute Press, Gorky (in Russian).

Pelinovsky, E.N., Troshina, E.N., 1994. Propagation of long waves in straits. Physics of Oceanography 5 (1), 43–48.

Rudenko, O., Soluyan, S., 1977. Theoretical Background of Nonlinear Acoustics. Plenum, New York.

Stoker, J.J., 1957. Water Waves. Wiley-Interscience, New York.

Tan, W.Y., 1992. Shallow Water Hydrodynamics. Elsevier, New York.

Tsuji, Y., Yanuma, T., Murata, I., Fujiwara, C., 1991. Tsunami ascending in rivers as an undular bore. Natural Hazards 4, 257–266.

Voltsinger, N.E., Klevanny, K.A., Pelinovsky, E.N., 1989. Long Wave Dynamics of the Coastal Zone. Hydrometeoisdat, Leningrad (in Russian).

Whitham, G.B., 1974. Linear and Nonlinear Waves. Wiley, New York.

Wu, Y.H., Tian, J.-W., 2000. Mathematical analysis of long-wave breaking on open channels with bottom friction. Ocean Engineering 26, 187–201.

Zahibo, N., Pelinovsky, E., Talipova, T., Kozelkov, A., Kurkin, A., 2006. Analytical and numerical study of nonlinear effects at tsunami modelling. Applied Mathematics and Computation 174, 795–809.